

Implementation of discrete least squares meshless method for nonlocal elastic graphene nanoplates

M.J. Rahi^a, A.R. Firoozjaee^a and M. Dehestani^{a*}

^aFaculty of Civil Engineering, Babol Noshirvani University of Technology, Babol, Iran

ARTICLE INFO

Article history:

Received 10 January, 2018

Accepted 4 June 2018

Available online

4 June 2018

Keywords:

Graphene

Rectangular nanoplate

Nonlocal elasticity theory

DLSM

ABSTRACT

In this paper, armchair rectangular monolayer graphene nanoplates were analyzed based on the assumption of orthotropic properties with different boundary conditions. For this purpose, the nonlocal elasticity and Kirchhoff theories were applied to analyze the small-scale effects on the armchair monolayer graphene nanoplates and obtain the static equation of the graphene nanoplates, respectively. As there were no readily accurate answers to the analyses of all the problems associated with nanoplates of different boundary and geometrical conditions, numerical methods were employed for obtaining approximate responses. One of the capable approaches to the analyses of the differential equations governing these types of plates is the meshless method. In this research, the Discrete Least Squares Meshless (DLSM) method was employed for the static analysis of rectangular nanoplates with different boundary conditions besides assessing the effect of nonlocal coefficient amount on the nanoplate deflection. According to the results of this investigation, it could be concluded that the method utilized here was suitable for solving the problems of nano-dimensions compared to the analytical and Galerkin meshless methods.

© 2018 Growing Science Ltd. All rights reserved.

1. Introduction

One of the sciences of the new era is nanotechnology and a key part of this science is to find the physical behaviors of nanomaterials, which is a new approach of all fields and technologies. The unique (mechanical, electrical, and even chemical) characteristics of nanomaterials have led to a rapid growth in this science. Graphene plates belonging to the classification of nanolayers have been developed from the juxtaposition of carbon atoms in a plate and crystal network with hexagonal structures. These structures make the different angles of carbon-carbon bonds with intraplate charges across various directions, thus having orthotropic properties. Due to the presence of a strong covalent force between carbon atoms despite their trivial thickness, they have a tensile strength of 200 times larger than that of a steel structure. Carbon nanoplates are classified into the 2 monolayer and multilayer groups. In the multilayer graphene nanoplates, there is a weak Van der Waals force between each layer. Monolayer plates are superior in many cases and further used compared to their multilayer counterparts; however, in cases that the bending strength enhancement is aimed at, a multilayer graphene sheet can be applied. Graphene nanoplates are classified into the 3 armchair, zigzag, and chiral (asymmetrical) groups in terms of rolling, each of which gives unique structural properties to the graphene plates.

* Corresponding author. Tel: +989113136113
E-mail addresses: dehestani@nit.ac.ir (M. Dehestani)

Graphene plates have a wide range of applications in a variety of nano-stimulants, nanosensors, electric batteries, and generally the compartments used in nano- and micro-electromechanical systems, anatomic force microscopes, and composites to enhance their strengths (Geim et al., 2007; Pumera et al., 2010; Geim, 2009; Katsnelson, 2007; Rao et al., 2009; Heyrovská, 2008; Choi et al., 2010; Geim et al., 2008; Chen et al., 2008; Kuzmenko et al., 2008; Zhang et al., 2015). All these applications besides the special characteristics of these plates have attracted researchers' attentions. One of the aspects of interest is the mechanical properties of graphene plates. Using different theoretical and experimental methods, researchers have tried to find their properties. However, experimental methods are very demanding, time-consuming, and costly. On the other hand, numerical and theoretical methods help to save time and costs and bring about desirable results (Martel et al., 1998).

To examine the mechanical properties of graphene plates and generally inspect small-scaled materials, the classical continuum theory has a big disadvantage. The problem is that at this scale, the void spaces between the atoms and atomic forces among the particles cannot be neglected with respect to the main dimensions and physics of the problem. In larger structures, creation of a resultant stress at a point is corresponding to the strain at that point. However, in nanostructures, the resultant stress is also dependent on the strain of the space surrounding that point. Therefore, other methods including experimental observations and molecular dynamics should be also taken into account (Eringen, 1972; Eringen, 1983; Eringen, 2002). Nevertheless, these approaches are very costly, time-consuming, and limited to low atom numbers in the structures. To demonstrate this dependence and remove this disadvantage, various theories have been presented including strain gradient (Fleck et al., 1997), modified couple stress (Yang et al., 2002), and micropolar (Nowacki, 1974) and nonlocal elasticity (Eringen, 1983; Jomehzadeh & Saidi, 2011; Zenkour & Sobhy, 2013) theories. In the nonlocal elasticity theory, there is a possibility of applying the internal characteristic length, i.e., the way the connections are established in the molecular network regarding particle dimensions, etc., along with the external characteristic lengths of the nanostructures, including the lengths of cracks, wavelength, etc. This method brings about acceptable results close to those of the atomic and molecular dynamic method (Duan & Wang, 2009; Wang et al., 2006; Alzahrani et al., 2013).

In the studies conducted on graphene plates, Ansari et al. (2010a) presented a vibrational analysis of monolayer graphene sheets using the nonlocal elasticity equations, classical plate theory, and general differential equations. Also, they dealt with the study of superficial stress based on the free vibration behaviors of nanoplates. They concluded that the effects of superficial stress for non-classical plate models can be neglected for fewer modes and higher dimension ratio values. Pardhan and Fadicare (2009) obtained the equations of movement based on the nonlocal theory by using the classical plate and first-order shear-transformation-zone theories. Finally, they solved the equations using the Navier-Stokes method and obtained the vibrations of graphene plates. Samaei et al. (2015) studied the effect of length scale on the vibration response of a single-layer graphene sheet embedded in an elastic medium using nonlocal Mindlin plate theory. Ansari et al. (2010b) used the finite element method and studied the vibrations of multilayer graphene sheets placed in an elastic medium with different boundary conditions.

Recently, various studies have been conducted on the bending, buckling, and vibrations of monolayer and multilayer graphene sheets by Sobhi (2014), Zankour et al. (2013) using the fourth-order differential method, Murmu and Pardhan (2009) investigated the buckling behaviors of elastic small-scale orthotropic plates under the influence of biaxial stress. Malekzadeh et al. (2011a,b) researched the vibrational and thermal buckling behavior of a desired tetrahedral orthotropic nanoplate. Sakhaipour et al. (2008) applied the molecular structure mechanics and modeled the vibrational behaviors of armchair and zigzag monolayer graphene plates with different boundary conditions. Don and Wang (2009) utilized a molecular mechanics simulation and investigated nonlinear bending and stretching of a circular graphene plate under a point load at the center. Aghababaei and Redi (2009) and Reddy (2010) provided a reformulation based on the third-order shear-transformation-zone of the

plate theory for the bending and vibration problems by using Eringen's nonlocal elasticity theory. Babaee and Shahidi (2011) studied the buckling behaviors of elastic tetrahedral monolayer graphene sheets under the influence of biaxial pressure using Galerkin method and nonlocal continuum mechanics. Jame'ezadeh and Sa'eedi (2011) investigated graphene sheets through a 3D vibration analysis by using the separation field equations of Eringen's nonlocal elasticity theory. Pradhan and Murmu (2009) by applying nonlocal Timoshenko beam theory and the fourth-order differential method, they benefited from the stability analysis of monolayer carbon nanotubes embedded in the elastic medium. Peddieson et al. (2003) first studied the small-scale effects on nanoscale structures by using the nonlocal elasticity theory. They showed that the nonlocal continuum mechanics has a high potential to be used in nanotechnology applications. Similarly, in another work, Behfar et al. (2006) utilized the analytical methods to investigate and calculate the bending modulus of bilayer graphene sheets. Sakhaeepour (2009) investigated the elastic properties of monolayer graphene sheets. Using the analytical methods, he managed to obtain Young's modulus, shear modulus, and Poisson's ratio for different types of carbon-atom arrangements in the mentioned plates. They concluded that the small-scale effects are completely scientific and should be taken into consideration. In another work, Redi (2010) obtained nonlinear bending for nanotubes and orthotropic plates by using the relations of beams and the classic theory together with the first-order sheer deformation theory based on the nonlocal effects, respectively.

Shen et al. (2010) investigated the nonlinear vibration of monolayer graphene placed in a thermal environment for the analysis of orthotropic rectangular plates with simple boundary conditions. In another work, Shen (2011) dealt with the nonlinear investigation and analysis of thin bands placed on an elastic support in a thermal environment based on the plate nonlocal model. Pouresmaeli et al. (2012) investigated the free vibrations of bilayer rectangular nanoplates in a polymer environment. Farajpour et al. (2012) studied the buckling of monolayer graphene plates undergoing a wide range of intraplate linear loads using the nonlocal theory and Moving Least Squares Differential Quadrature (MLSDQ) method. To validate the results, they solved the equations by using a power series method and concluded that the results of both methods were nearly similar. Zang et al. (2015) used the meshless method for the vibrational analysis of monolayer graphene sheets based on the continuum nonlocal method. Arash and Wang (2011) utilized an analytical method for the vibrational investigation of monolayer and multilayer graphene sheets. Naderi and Baradaran (2013) applied Galerkin meshless method for the static analysis of microscale nanoplates based on the nonlocal plate theory with different boundary conditions.

In this research, for the static analysis of armchair graphene nanoplates, the nonlocal elasticity theory was used assuming that the thickness of the nanoplate is negligible relative to other dimensions. To develop the nanoplate static equation, Kirchhoff theory was utilized and a DLSM numerical method was applied through a Moving Least Square (MLS) approximation for estimating the shape functions since it was difficult to solve the mechanical problems of nanostructures with different boundary conditions. So far, this method has not been employed for the mechanical analysis of nanostructures, which was successfully used in this paper. The results obtained by this research can be useful for recognizing the practical characteristics of this type of structures.

2. Nonlocal elasticity theory

Nonlocal elasticity theory is defined regarding the fact that stress at point x is from a continuous body of a strain function across all x' points of the body (Eringen, 1983). Therefore, nonlocal stress is expressed as follows:

$$\sigma_{ij} = \int_V \lambda(|x - x'|) C_{ijkl} \varepsilon_{kl} dv(x') \quad (1)$$

where σ_{ij} is the nonlocal stress; λ represents the kernel function; $|x - x'|$ is the Euclidean form of the distance between x and x' ; ε_{kl} denotes the strain; and C_{ijkl} is the elasticity tensor.

Using Eq. (1) in the moving equation, we have:

$$\sigma_{ij} + f_i = \rho \ddot{u}_i \quad (2)$$

where f_i , \ddot{u}_i , and ρ represent the body force, displacement vector, and mass density, respectively. Eq. (1) is then rewritten as the following:

$$\Gamma \sigma_{ij} = C_{ijkl} \varepsilon_{kl} \quad (3)$$

where Γ is the derivative operator. Hence, the equation of movement can be written as follows:

$$(C_{ijkl} \varepsilon_{kl})_j + \Gamma(f_i - \rho \ddot{u}_i) = 0 \quad (4)$$

Eq. (4) is a partial differential equation with a simple form of partial integral equations. This form is then utilized in the nonlocal elasticity theory.

For the 2D problems, we have:

$$\Gamma = 1 - \mu \nabla^2 \quad (5)$$

where

$$\lambda(|x|) = (2\pi L^2 \tau^2)^{-1} k_0(|x|/L\tau) \quad \tau = e_0 a_0 / L \quad (6)$$

where

$$\int_V \lambda(|x|) dV = 1 \quad (7)$$

where ∇^2 , k_0 , a_0 and L denote Laplacian operator, Bessel function, and the internal and external properties of the length, respectively given that $\mu = (e_0 a_0)^2$, in which e_0 is both theoretically and experimentally estimated by using the models of elasticity theory. τ is material constant.

Using Eq. (3) to Eq. (7), the differential form of the nonlocal elasticity is written as follows:

$$\left(1 - \mu \left(\frac{\partial^2}{\partial x^2} + \frac{\partial^2}{\partial y^2}\right)\right) \sigma_{ij} = C_{ijkl} \varepsilon_{kl} \quad (8)$$

which eventually culminates in the following statements (Analooei et al., 2013):

$$(1 - \mu \nabla^2) \sigma_{ij} = C_{ijkl} \varepsilon_{kl} \quad (9)$$

$$(1 - (e_0 a_0)^2 \nabla^2) \sigma_{ij} = \sigma^L \quad (10)$$

where σ^L is the local stress.

3. Equilibrium equation

Assuming that the rectangular orthotropic thin plates have a length, width, thickness, and lateral load of a , b , h , and $p(x, y)$, respectively, based on Kirchhoff plate theory, the strain-displacement equation of the plate in Cartesian coordinates is written as follows:

$$\begin{Bmatrix} \varepsilon_x \\ \varepsilon_y \\ \gamma_{xy} \end{Bmatrix} = \begin{Bmatrix} -zw_{,xx} \\ -zw_{,yy} \\ -2zw_{,xy} \end{Bmatrix} \quad (11)$$

where w is the lateral displacement of the middle plate, " $,$ " refers to the partial derivatives, and z is the axis in the direction of the plate thickness. The equations constituting an orthotropic plate are written as follows:

$$\begin{Bmatrix} \sigma_x \\ \sigma_y \\ \tau_{xy} \end{Bmatrix} - (e_0 a_0)^2 \nabla^2 \begin{Bmatrix} \sigma_x \\ \sigma_y \\ \sigma_{xy} \end{Bmatrix} = \begin{Bmatrix} \bar{Q}_{11} & \bar{Q}_{12} & \bar{Q}_{16} \\ \bar{Q}_{12} & \bar{Q}_{22} & \bar{Q}_{26} \\ \bar{Q}_{16} & \bar{Q}_{26} & \bar{Q}_{66} \end{Bmatrix} \begin{Bmatrix} \varepsilon_x \\ \varepsilon_y \\ \gamma_{xy} \end{Bmatrix} \quad (12)$$

where \bar{Q}_{ij} 's ($i, j = 1, 2, 6$) are reduced off-axis stiffness defined in terms of the reduced on-axis Q_{ij} 's as (Naderi et al., 2013).

$$\begin{Bmatrix} \bar{Q}_{11} \\ \bar{Q}_{12} \\ \bar{Q}_{16} \\ \bar{Q}_{22} \\ \bar{Q}_{26} \\ \bar{Q}_{66} \end{Bmatrix} = \begin{Bmatrix} c^4 & 2c^2s^2 & s^4 & 4c^2s^2 \\ c^2s^2 & c^4+s^4 & c^2s^2 & -4c^2s^2 \\ c^3s & cs^3-c^3s & -cs^3 & -2cs(c^2-s^2) \\ s^4 & c^2s^2 & c^4 & 4c^2s^2 \\ cs^3 & c^3s-cs^3 & -c^3s & 2cs(c^2-s^2) \\ c^2s^2 & -2c^2s^2 & c^2s^2 & (c^2-s^2)^2 \end{Bmatrix} \begin{Bmatrix} Q_{11} \\ Q_{22} \\ Q_{12} \\ Q_{12} \\ Q_{66} \end{Bmatrix} \quad (13)$$

where $s = \sin(\theta)$, $c = \cos(\theta)$, and Q_{ij} are defined as the following engineering constants:

$$\begin{aligned} Q_{11} &= \frac{E_1}{(1-v_{12}v_{21})}, Q_{22} = \frac{E_2}{(1-v_{12}v_{21})}, \\ Q_{12} &= \frac{v_{12}E_1}{(1-v_{12}v_{21})}, Q_{66} = G_{12}. \end{aligned} \quad (14)$$

θ is the external axial angle, which is 0° and 90° for the armchair and zigzag graphene nanoplates. Using the principle of virtual work, the plate equilibrium equation is obtained as follows:

$$\frac{\partial^2 M_x}{\partial x^2} + 2 \frac{\partial^2 M_{xy}}{\partial x \partial y} + \frac{\partial^2 M_y}{\partial y^2} + p(x, y) = 0 \quad (15)$$

where the nonlocal moments of M_x , M_y , and M_{xy} are defined as follows:

$$\begin{Bmatrix} M_x \\ M_y \\ M_{xy} \end{Bmatrix} - (e_0 a_0)^2 \nabla^2 \begin{Bmatrix} M_x \\ M_y \\ M_{xy} \end{Bmatrix} = \begin{Bmatrix} M_x^L \\ M_y^L \\ M_{xy}^L \end{Bmatrix} \quad (16)$$

M_x^L , M_y^L , and M_{xy}^L are the results of the local moments expressed as follows:

$$\begin{Bmatrix} M_x^L \\ M_y^L \\ M_{xy}^L \end{Bmatrix} = \begin{Bmatrix} D_{11} & D_{12} & D_{16} \\ D_{12} & D_{22} & D_{26} \\ D_{16} & D_{26} & D_{66} \end{Bmatrix} \begin{Bmatrix} w_{,xx} \\ w_{,yy} \\ w_{,xy} \end{Bmatrix} \quad (17)$$

where $D_{ij} = \int_{-h/2}^{h/2} z^2 \bar{Q}_{ij} dz$ ($i, j = 1, 2, 6$). Using Eq. (15) and Eq. (16), the following equation is obtained:

$$\frac{\partial^2 M_x^L}{\partial x^2} + 2 \frac{\partial^2 M_{xy}^L}{\partial x \partial y} + \frac{\partial^2 M_y^L}{\partial y^2} + (1 - (e_0 a_0)^2 \nabla^2) p(x, y) = 0. \quad (18)$$

The boundary conditions at each side of the plate are as follows:

For simply supported:

$$w = M_n = 0 \quad (19)$$

For clamped supported:

$$w = w_n = 0 \quad (20)$$

Free edges:

$$V_n = M_n = M_{nt} = 0 \quad (21)$$

Here, V is shear force; n is the normal vector at the boundary and t is the tangential vector in the plate. The analytical solutions are limited for the problem of plate bending based on the nonlocal theory of simple-support plates (Lu et al., 2007). Therefore, for plates with different boundary conditions, numerical methods along with the DLSM method are required to solve the equilibrium Eq. (17) and Eq. (18) by combining the boundary conditions (19-21) based on Fig. 1.

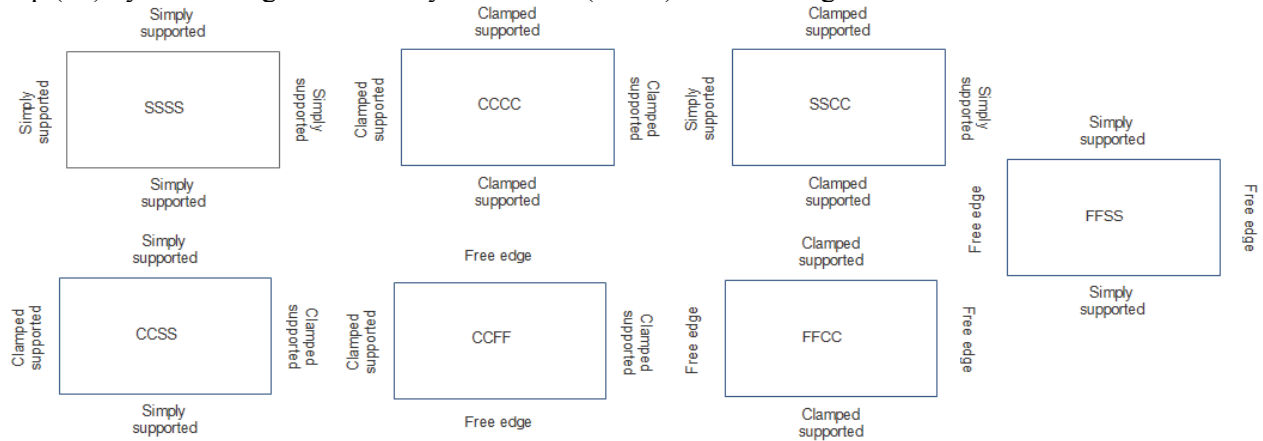


Fig. 1. Different boundary conditions of graphene nanoplates.

4. Analysis of shape functions using MLS

In the DLSM method, shape functions are generated by MLS. An MLS-based estimation enjoys two prominent features, which lead to its popularity: (1) the approximate field function throughout the entire range of the problem is continuous and smooth; and (2) it has the ability of developing the approximation with a desired order of compatibility (Liu, 2009). Here, $\Phi(X)$ is the estimated function at the point of $X = [x, y]$.

$$\Phi(X) = \sum_{i=1}^{mp} p_i(X) a_i(X) = P^T(X) a(X) \quad (22)$$

where $p_i(X)$ is the vector of Polynomial Basis Functions (PBFs) in the spatial coordinates, mp shows the number of the statements of the basis functions, and $a(X)$ is the vector of coefficients. The first-order and second-order polynomial basis functions in the 1D and 2D states can be specified as follows: $P^T = [1 \ x]$ for basis of first order in one dimension, $P^T = [1 \ x \ y]$ for basis of 1st order in two dimensions, $P^T = [1 \ x \ x^2]$ for basis of 2nd order in one dimension and $P^T = [1 \ x \ y \ x^2 \ xy \ y^2]$ for basis of 2nd order in two dimensions, where x and y represent the first and second elements of spatial coordinates.

Note that $a(X)$ in Eq. (22) is a function of X and by minimizing $J(X)$ function, it can be obtained as shown below:

$$J(X) = \sum_{j=1}^n W(X - X_j)(P^T(X_j)a(X) - \Phi_j^h)^2 \quad (23)$$

where $W(X - X_j)$ is the weight function as one of the properties of the meshless method. Here, a third-order cubic spline function is used:

$$W(X - X_j) = W(\bar{d}) = \begin{cases} 2/3 - 4\bar{d}^2 + 4\bar{d}^3 & \bar{d} \leq 1/2 \\ 4/3 - 4\bar{d} + 4\bar{d}^2 - 4/3\bar{d}^3 & 1/2 \leq \bar{d} \leq 1 \\ 0 & \bar{d} > 1 \end{cases} \quad (24)$$

where $\bar{d} = |X - X_j|/dw_j$ and dw_j is the radius of influence of point X_j . By minimizing Function J , we have:

$$\Phi(X) = P^T(X)A^{-1}(X)B(X)\varphi^h \quad (25)$$

where φ^h is the nodal parameter vector, and $A(X)$ and $B(X)$ are exhibited as follows:

$$A(X) = \sum_{j=1}^n W(X - X_j)P(X_j)P^T(X_j) \quad (26)$$

$$B(X) = [W(X - X_1)P(X_1), W(X - X_2)P(X_2), \dots, W(X - X_n)P(X_n)] \quad (27)$$

Based on Eq. (24), the above equation can be rewritten as follows:

$$\Phi(X) = N^T(X)\varphi^h, \quad (28)$$

$$N^T(X) = P^T(X)A^{-1}(X)B(X), \quad (29)$$

where $N^T(X)$ represents the shape function vector for nodal elements at point X , which is called an MLS shape function.

5. DLSM method

To present a method from DLSM, the general form of the following differential equations is used for developing the system of discrete equations. The differential equations with their partial derivatives and boundary conditions are written as follows:

$$\Im(\Phi) + f = 0 \quad \text{in } \Omega \quad (30)$$

$$\Phi - \bar{\Phi} = 0 \quad \text{in } \Gamma_2 \quad (31)$$

$$\Re(\Phi) + \bar{t} = 0 \quad \text{in } \Gamma_1 \quad (32)$$

where Ω is the problem domain; Γ_1 , and Γ_2 are the Dirichlet and Neumann boundary conditions, respectively; \Im and \Re are the partial differential operators; and f represents the external force or the source term within the problem domain. The remaining value of the differential equation in a typical point K is as follows:

$$R_\Omega(X_k) = \Im(\Phi(X_k)) + f(X_k) = \sum_{j=1}^n \Im(N_j(X_k))\Phi_j + f(X_k), \quad (33)$$

$$K = 1, \dots, m \quad (34)$$

The remaining value of Neumann boundary conditions at the typical point K can be written as follows:

$$R_1(X_k) = \Re(\Phi) - \bar{t}(X_k) = \sum_{j=1}^n \Re(N_j(X_k))\Phi_j - \bar{t}(X_k) \quad (35)$$

$$K = 1, \dots, m_1 \quad (36)$$

Eventually, the remaining value of Dirichlet boundary conditions at the typical point K can be expressed as follows:

$$R_2(X_k) = \Phi - \bar{\Phi}(X_k) = \sum_{j=1}^n N_j(X_k)\Phi_j - \bar{\Phi}(X_k) \quad (37)$$

$$K = 1, \dots, m_2 \quad (38)$$

where n is the number of nodal points; m represents the number of sampling points in the domain; and m_1 and m_2 indicate the numbers of sample points chosen in the Dirichlet and Neumann boundaries, respectively. m_1 and m_2 are normally dependent on the number of the points of sample m though a greater number of these sample points develops a better correspondence for meeting the boundary conditions. A penalty method is utilized to develop the total remaining value of the problem:

$$I = \sum_{k=1}^m R_\Omega^2(X_k) + \alpha_1 \sum_{k=1}^{m_1} R_1^2(X_k) + \alpha_2 \sum_{k=1}^{m_2} R_2^2(X_k) \quad (39)$$

where α_1 and α_2 are the penalty coefficients for Dirichlet and Neumann boundary conditions, respectively. By combining the above equations, the following relation is obtained:

$$\begin{aligned} I &= \sum_{k=1}^m \left(\sum_{j=1}^n \Im(N_j(X_k))\Phi_j + f(X_k) \right)^2 + \\ &\quad \alpha_1 \sum_{k=1}^{m_1} \left(\sum_{j=1}^n \Re(N_j(X_k))\Phi_j - \bar{t}(X_k) \right)^2 + \\ &\quad \alpha_2 \sum_{k=1}^{m_2} \left(\sum_{j=1}^n N_j(X_k)\Phi_j - \bar{\Phi}(X_k) \right)^2 \end{aligned} \quad (40)$$

By minimizing Eq. (40), considering nodal parameters ($\Phi_j, j = 1, 2, 3, \dots, n$), and incorporating them into Eq. (41), Eq. (42) and Eq. (43) are achieved:

$$k \Phi = F \quad (41)$$

$$\begin{aligned} k_{ij} = & \sum_{k=1}^m \Im(N_i(X_k))\Im(N_j(X_k)) + \\ & \alpha_1 \sum_{k=1}^{m_1} \Re(N_i(X_k))\Re(N_j(X_k)) + \\ & \alpha_2 \sum_{k=1}^{m_2} N_i(X_k)N_j(X_k) \end{aligned} \quad (42)$$

$$\begin{aligned} F_i = & -\sum_{k=1}^m \Im(N_i(X_k))f(X_k) + \\ & \alpha_1 \sum_{k=1}^{m_1} \Re(N_i(X_k))\bar{t}(X_k) + \alpha_2 \sum_{k=1}^{m_2} N_i(X_k)\bar{\Phi}(X_k) \end{aligned} \quad (43)$$

Matrix k is symmetrical, which can be readily used to solve the problem (Firoozjaee et al., 2009).

6. Numerical example and the results

In this section, the DLSM method was implemented on a rectangular monolayer armchair graphene nanoplate with different boundary conditions. For validating the numerical solution, an accurate deflection solution was required for a thin graphene plate with the dimensions of a and b and thickness of h undergoing the following load:

$$f = f_{\lambda\mu} \sin(\zeta_\lambda x) \sin(\eta_\mu y) \quad (44)$$

where $\zeta_\lambda = \pi/a$ and $\eta_\mu = \pi/b$.

For a nanoplate with a simple support around it, an accurate deflection equation was obtained by using Eq. (17) and Eq. (18) as follows (Naderi et al., 2013):

$$w(x, y) = \frac{(1 + (e_0 a_0)^2 (\zeta_\lambda^2 + \eta_\mu^2))}{(D_{11} \zeta_\lambda^4 + 2(D_{12} + 2D_{66}) \zeta_\lambda^2 \eta_\mu^2 + D_{22} \eta_\mu^4)} \times f_{\lambda\mu} \sin(\zeta_\lambda x) \sin(\eta_\mu y) \quad (45)$$

Now, by having the analytical and numerical solutions for each node, the median error of er_0 can be obtained using the following relation (Firoozjaee et al., 2009):

$$er_0 = \frac{\sum_{i=1}^m |w_i^{exact} - w_i^{num}|}{\sum_{i=1}^m |w_i^{exact}|} \quad (46)$$

w_i^{exact} and w_i^{num} are the deflections of the points obtained from the analytical and numerical solutions and $i = 1, 2, \dots, m$ and m represent the total numbers of the sampling nodes.

Finally, deflection of the rectangular monolayer armchair graphene nanoplate with the following properties are obtained.

Armchair:

$$a = 9.519 \text{ nm}, b = 4.844 \text{ nm}, h = 0.129 \text{ nm}, e_0 a_0 = 0.67 \text{ nm}, E_1 = 2434 \text{ GPa}, E_2 = 2473 \text{ GPa},$$

$$\nu_{12} = 0.197, G_{12} = 1039 \text{ GPa}$$

where E_1, E_2, ν_{12} , and G_{12} are the elastic moduli, Poisson's coefficient, and shear modulus in the directions of x and y, respectively. The output results using Eq. (43) and DLSM method are presented in the Table 1, Table 2, and Table 3.

Table 1. The middle node deflection based on the accurate and estimated solutions ($e_0 a_0 = 0.67 \text{ nm}$, $\alpha_1 = 10^7$, $\alpha_2 = 10^0$, $S = 2$)

Edge condition SSSS						
N_x	N_y	$\Delta x, \text{nm}$	dw, nm	er_0	w, nm	w^{exact}, nm
11	11	0.951900	2.808105	0.0505	-9.1994	-9.5914
17	17	0.594938	1.7550671	0.0173	-9.4345	-9.5914
21	21	0.475950	1.4040525	0.0122	-9.4760	-9.5914
31	31	0.317300	0.936035	0.0085	-9.5110	-9.5914
41	41	0.237975	0.70202625	0.0080	-9.5158	-9.5914

Table 2. The middle node deflection based on the accurate and estimated solutions ($e_0 a_0 = 0.67 \text{ nm}$, $\alpha_1 = 10^7$, $\alpha_2 = 10^0$, $S = 3$)

Edge condition SSSS						
N_x	N_y	$\Delta x, \text{nm}$	dw, nm	er_0	w, nm	w^{exact}, nm
11	11	0.951900	2.808105	0.0500	-9.2029	-9.5914
17	17	0.594938	1.7550671	0.0139	-9.4623	-9.5914
21	21	0.475950	1.4040525	0.0091	-9.5051	-9.5914
31	31	0.317300	0.936035	0.0061	-9.5338	-9.5914
41	41	0.237975	0.70202625	0.0056	-9.5379	-9.5914

Here, S represents the number of the sampling points between every two main nodes; Δx denotes the distance between the two main nodes; and N_x is the number of the main nodes within the directions of x and N_y is the number of the main nodes within the directions of y coordinates. Figs. 2 and 3 demonstrate the sampling points and nodal points regularly distributed within the rectangular computational range. For the analysis of the problem, a regular network of the sampling points was applied.

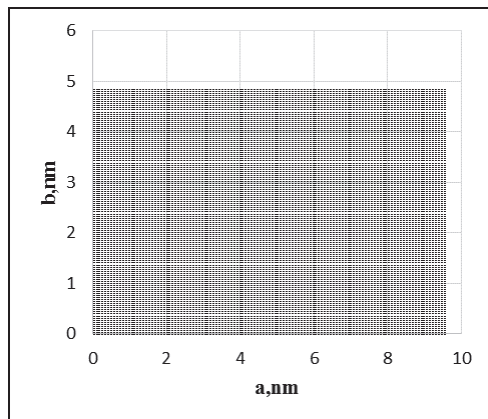


Fig. 2. Regular distribution of the sampling points

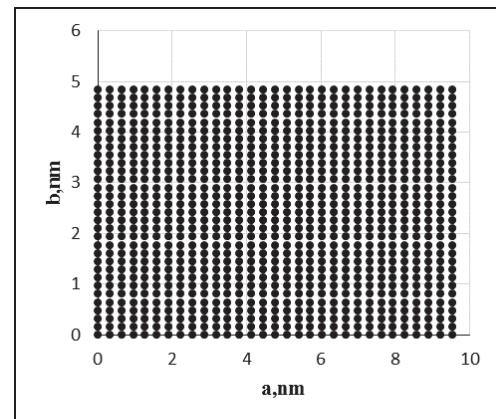


Fig. 3. Regular distribution of the nodal points

Fig. 4 depicts the fact that with an increase in the number of the sampling points, the amount of error declines with a greater rate.

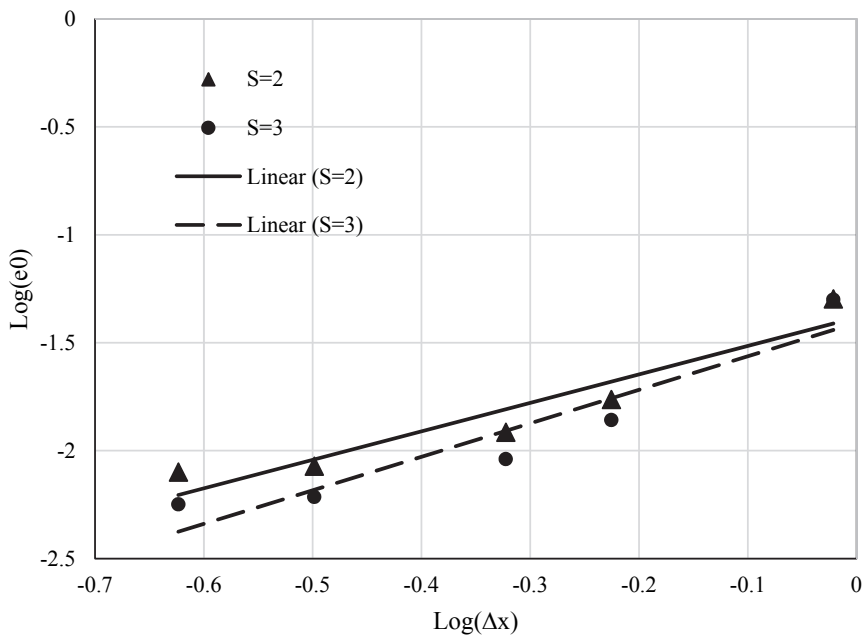


Fig. 4. The effect of an increase in the number of the sampling points as many as $N_x = N_y = 31$ on the median error for the nodal points with SSSS boundary conditions

$$(e_0 a_0 = 0.67 \text{ nm}, dw = 0.936035 \text{ nm}, \alpha_1 = 10^7, \alpha_2 = 10^0)$$

Fig. 5 displays a comparison of the plate deflection between the DLSM numerical method and analytical method. The extent of correspondence between the two relevant diagrams suggests that the numerical method used in this paper is a very suitable method for solving this problem.

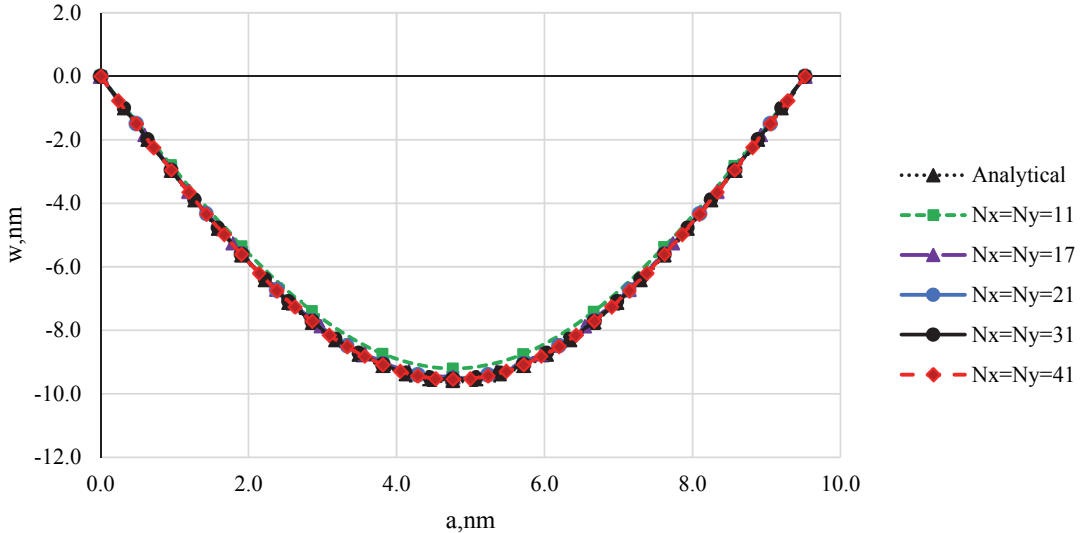


Fig. 5. Comparison of the results of the nanoplate deflection between the two numerical DLSM and analytical methods using the constancy of the sampling points with SSSS boundary conditions

$$(S = 3, e_0 a_0 = 0.67 \text{ nm}, dw = 0.936035 \text{ nm}, \alpha_1 = 10^7, \alpha_2 = 10^0)$$

Fig. 6 portrays the transformation of nanoplates using an analytical method for the boundary conditions around a simple support and Fig. 7 exhibits the transformation and 3D static deflection of the rectangular plate with the boundary conditions around a simple support by using the DLSM method.

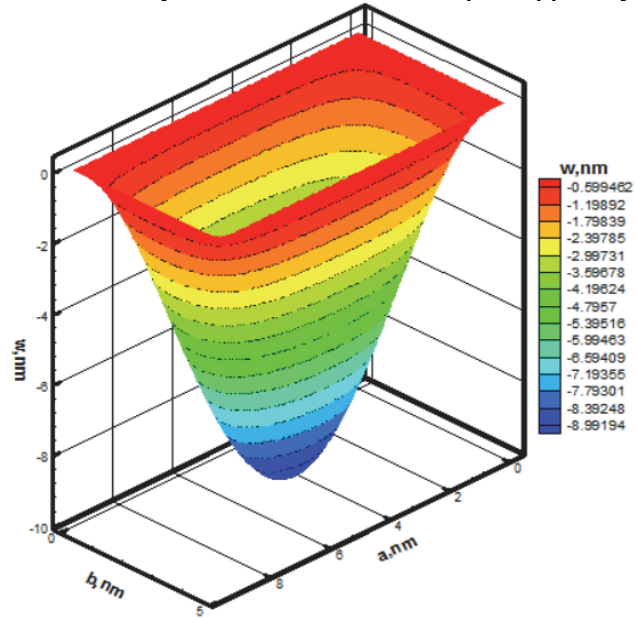


Fig. 6. The nanoplate deflection based on SSSS boundary conditions ($e_0 a_0 = 0.67 \text{ nm}$) using an analytical method

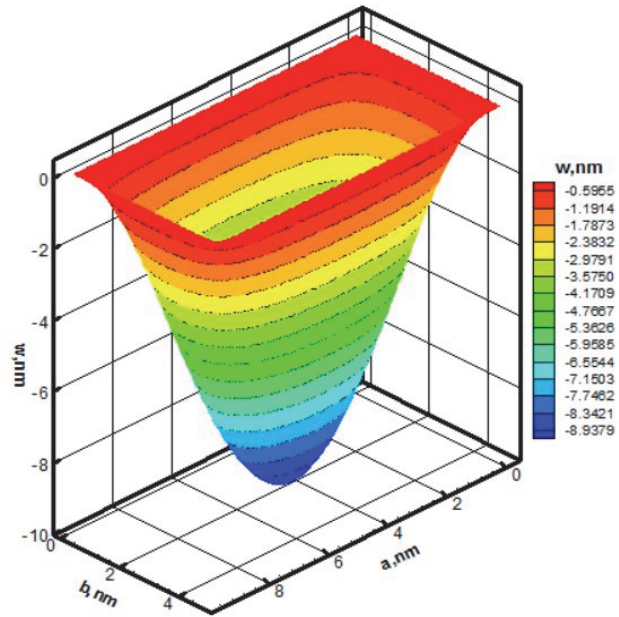


Fig. 7. The nanoplate deflection using the DLSM numerical method for SSSS boundary conditions ($N_x = N_y = 31, e_0 a_0 = 0.67 \text{ nm}, dw = 0.936035 \text{ nm}, \alpha_1 = 10^7, \alpha_2 = 10^0$)

In Fig. 8, the effects of the nonlocal coefficient on the deflection have been displayed, which actually present a comparison between the local and nonlocal analysis conditions. Then, a numerical solution has been studied with different boundary conditions. In Table 3, with an increase in the number of nodes, the extent of the plate deflection has grown with the boundary conditions around a clasped support and approached an accurate solution.

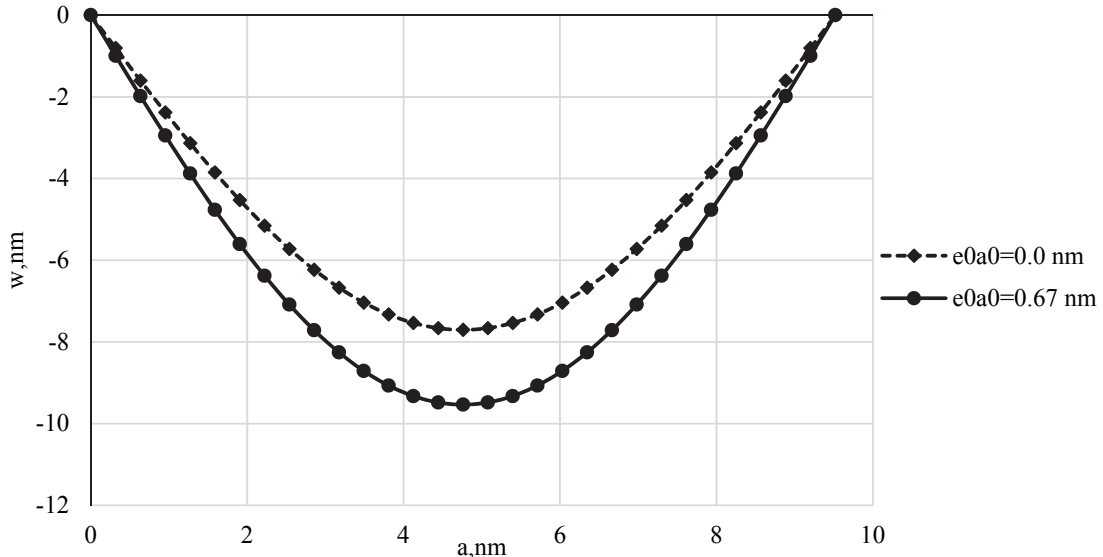


Fig. 8. Comparison of the transformation of the nanoplate deflections for SSSS boundary conditions with and without the nonlocal coefficient based on $N_x = N_y = 31$ nodal points by using the DLSM numerical method

Table 3. The middle node deflection based on estimated solutions ($e_0 a_0 = 0.67 \text{ nm}$, $\alpha_1 = 10^{14}$, $\alpha_2 = 10^{14}$, $S = 3$)

Edge condition CCCC				
N_x	N_y	$\Delta x, \text{nm}$	dw, nm	w, nm
11	11	0.951900	2.37975	-0.6256
17	17	0.594938	1.487345	-2.4589
21	21	0.475950	1.189875	-2.5696
31	31	0.317300	0.79325	-2.7227
41	41	0.237975	0.5949375	-2.7743

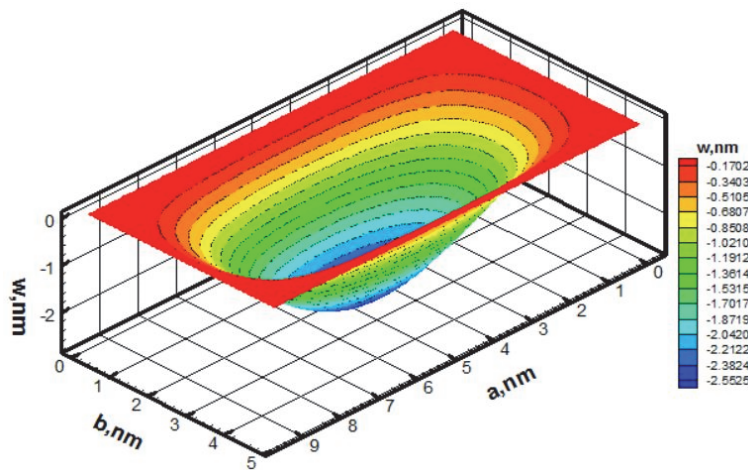


Fig. 9. The nanoplate deflection considering the DLSM numerical method with CCCC boundary conditions ($N_x = N_y = 31$, $e_0 a_0 = 0.67 \text{ nm}$, $dw = 0.79325 \text{ nm}$, $\alpha_1 = 10^{14}$, $\alpha_2 = 10^{14}$)

In Fig. 9, the transformation and 3D static deflection of the plate with the boundary conditions around a clasped support have been well represented by using the DLSM method. In Fig. 9 to Fig.15, variations in the deflection relative to the different boundary conditions of the nanoplate have been demonstrated via 3D diagrams by using the DLSM numerical method. In Fig. 10, the diagram of the plate deflection has been presented with the nonlocal coefficient for CCCC support conditions.

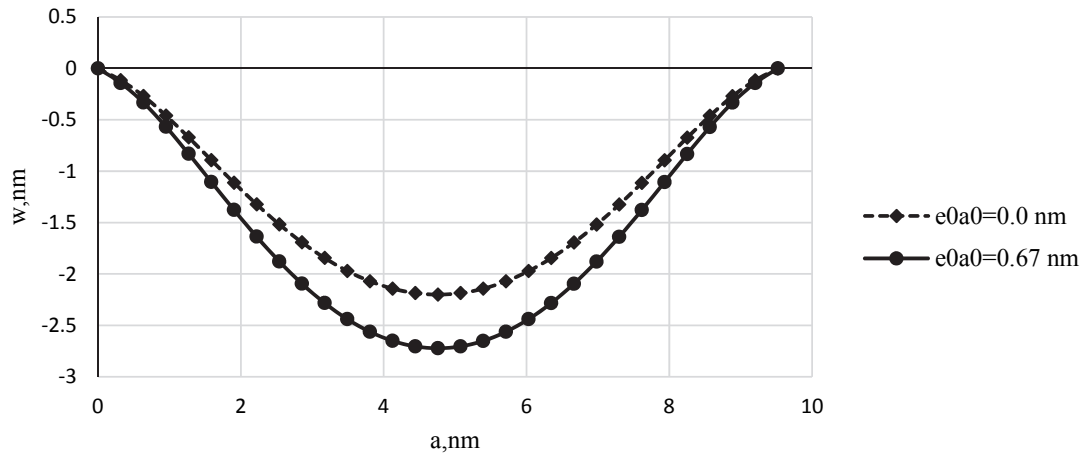


Fig. 10. Comparison of the nanoplate deflection transformation for CCCC boundary conditions with and without the nonlocal coefficient based on $N_x = N_y = 31$ nodal points by using the DLSM method

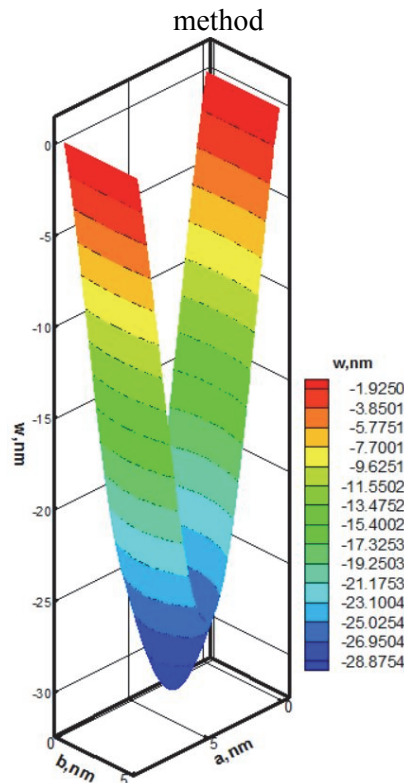


Fig. 11. The deflection of the armchair graphene nanoplate using the DLSM method with CCFF boundary conditions

$$(N_x = N_y = 31, e_0 a_0 = 0.67 \text{ nm}, d_w = 0.98363 \text{ nm}, \alpha_1 = 10^{11}, \alpha_2 = 10^{11})$$

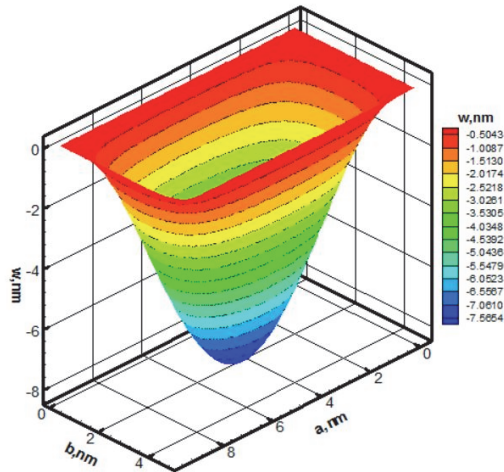


Fig. 12. The nanoplate deflection using the DLSM method with CCSS boundary conditions ($N_x = N_y = 31, e_0 a_0 = 0.67 \text{ nm}, dw = 0.72979 \text{ nm}, \alpha_1 = 10^{10}, \alpha_2 = 10^{10}$)

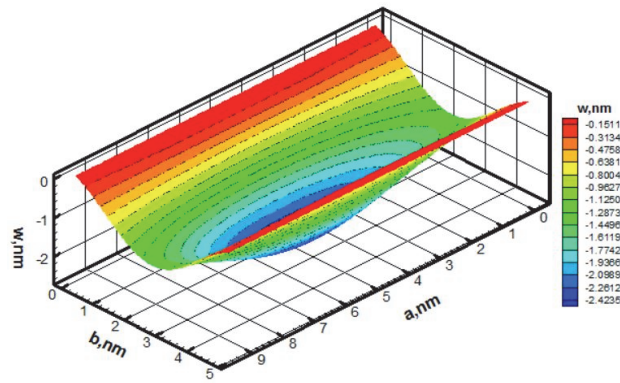


Fig. 13. The nanoplate deflection using the DLSM method with FFCC boundary conditions ($N_x = N_y = 31, e_0 a_0 = 0.67 \text{ nm}, dw = 0.60287 \text{ nm}, \alpha_1 = 10^7, \alpha_2 = 10^7$)

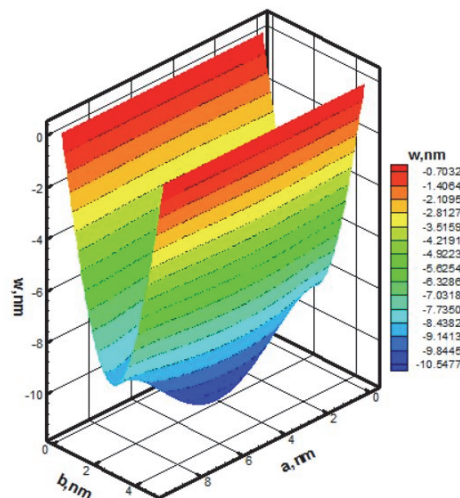


Fig. 14. The nanoplate deflection using the DLSM method with FFSS boundary conditions ($N_x = N_y = 31, e_0 a_0 = 0.67 \text{ nm}, dw = 0.9519 \text{ nm}, \alpha_1 = 10^{12}, \alpha_2 = 10^{12}$)

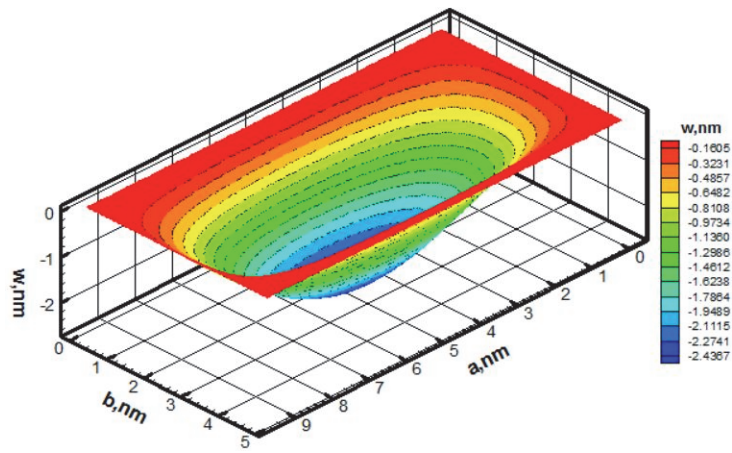


Fig. 15. The nanoplate deflection using the DLSM method with SSCC boundary conditions

$$(N_x = N_y = 31, e_0 a_0 = 0.67 \text{ nm}, dw = 0.69806 \text{ nm}, \alpha_1 = 10^{11}, \alpha_2 = 10^{11})$$

Table 4 provides the nanoplate deflection obtained for the different boundary conditions by using the DLSM and EFG methods.

Table 4. Comparison of the middle point deflections of the nanoplate (nm) obtained via the DLSM and EFG methods

Numerical methods	SSSS	CCCC	CCSS	SSCC	CCFF	FFCC	FFSS
EFG (Naderi et al. 2013)	9.8817	2.9229	8.5005	2.9831	31.7889	2.9831	11.6059
DLSM	9.5338	2.7227	8.0697	2.5993	30.8005	2.5858	11.2509

7. Conclusion

The results of the numerical method using the DLSM approach were in well congruence with the analytical results of the nanoplate problem, while the most suitable number of nodes for solving the mentioned nanoplate was 961 main nodes regularly distributed within a particular range with 3 nodes as the sampling points between each main node. Moreover, the deflection obtained by the DLSM method was in a good correspondence with that obtained by the EFG approach. Considering the fact that the nonlocal conditions of the nanoplate deflection were greater than those of the local state, the effects of the internal and external properties of the nanomaterials on the mechanics of the nanostructures were considerable due to the small dimensions as evidenced by the differences of deflections in this problem. Thus, it is concluded that the DLSM method is a suitable approach for solving nanoscale problems. Furthermore, nonlocal conditions should be applied to the differential equations governing the nano-problems.

Reference

- Aghababaei, R., & Reddy, J. N. (2009). Nonlocal third-order shear deformation plate theory with application to bending and vibration of plates. *Journal of Sound and Vibration*, 326(1-2), 277-289.
- Alzahrani, E. O., Zenkour, A. M., & Sobhy, M. (2013). Small scale effect on hygro-thermo-mechanical bending of nanoplates embedded in an elastic medium. *Composite Structures*, 105, 163-172.
- Analooei, H. R., Azhari, M., & Heidarpour, A. (2013). Elastic buckling and vibration analyses of orthotropic nanoplates using nonlocal continuum mechanics and spline finite strip method. *Applied Mathematical Modelling*, 37(10-11), 6703-6717.
- Ansari, R., Rajabiehfard, R., & Arash, B. (2010a). Nonlocal finite element model for vibrations of embedded multi-layered graphene sheets. *Computational Materials Science*, 49(4), 831-838.
- Ansari, R., Sahmani, S., & Arash, B. (2010b). Nonlocal plate model for free vibrations of single-layered graphene sheets. *Physics Letters A*, 375(1), 53-62.

- Arash, B., & Wang, Q. (2011). Vibration of single-and double-layered graphene sheets. *Journal of Nanotechnology in Engineering and Medicine*, 2(1), 011012.
- Babaei, H., & Shahidi, A. R. (2011). Small-scale effects on the buckling of quadrilateral nanoplates based on nonlocal elasticity theory using the Galerkin method. *Archive of Applied Mechanics*, 81(8), 1051-1062.
- Behfar, K., Seifi, P., Naghdabadi, R., & Ghanbari, J. (2006). An analytical approach to determination of bending modulus of a multi-layered graphene sheet. *Thin Solid Films*, 496(2), 475-480.
- Chen, J. H., Jang, C., Xiao, S., Ishigami, M., & Fuhrer, M. S. (2008). Intrinsic and extrinsic performance limits of graphene devices on SiO₂. *Nature nanotechnology*, 3(4), 206.
- Choi, W., Lahiri, I., Seelaboyina, R., & Kang, Y. S. (2010). Synthesis of graphene and its applications: a review. *Critical Reviews in Solid State and Materials Sciences*, 35(1), 52-71.
- Duan, W. H., & Wang, C. M. (2009). Nonlinear bending and stretching of a circular graphene sheet under a central point load. *Nanotechnology*, 20(7), 075702.
- Eringen, A. C. (1972). Nonlocal polar elastic continua. *International journal of engineering science*, 10(1), 1-16.
- Eringen, A. C. (1983). On differential equations of nonlocal elasticity and solutions of screw dislocation and surface waves. *Journal of applied physics*, 54(9), 4703-4710.
- Eringen, A. C. (2002). *Nonlocal continuum field theories*. Springer Science & Business Media.
- Eringen, A. C., & Edelen, D. G. B. (1972). On nonlocal elasticity. *International Journal of Engineering Science*, 10(3), 233-248.
- Farajpour, A., Shahidi, A. R., Mohammadi, M., & Mahzoon, M. (2012). Buckling of orthotropic micro/nanoscale plates under linearly varying in-plane load via nonlocal continuum mechanics. *Composite Structures*, 94(5), 1605-1615.
- Firoozjaee, A. R., & Afshar, M. H. (2009). Discrete least squares meshless method with sampling points for the solution of elliptic partial differential equations. *Engineering analysis with boundary elements*, 33(1), 83-92.
- Fleck, N. A., & Hutchinson, J. W. (1997). Strain gradient plasticity. *Advances in Applied Mechanics*, 33, 296-361.
- Geim, A. K. (2009). Graphene: status and prospects. *science*, 324(5934), 1530-1534.
- Geim, A. K., & Kim, P. (2008). Carbon wonderland. *Scientific American*, 298(4), 90-97.
- Geim, A. K., & Novoselov, K. S. (2007). The rise of graphene. *Nature materials*, 6(3), 183.
- Heyrovská, R. (2008). Atomic structures of graphene, benzene and methane with bond lengths as sums of the single, double and resonance bond radii of carbon. *arXiv preprint arXiv:0804.4086*.
- Jomehzadeh, E., & Saidi, A. R. (2011). Decoupling the nonlocal elasticity equations for three dimensional vibration analysis of nano-plates. *Composite Structures*, 93(2), 1015-1020.
- Katsnelson, M. I. (2007). Graphene: carbon in two dimensions. *Materials today*, 10(1-2), 20-27.
- Kuzmenko, A. B., Van Heumen, E., Carbone, F., & Van Der Marel, D. (2008). Universal optical conductance of graphite. *Physical review letters*, 100(11), 117401.
- Liu, G. R. (2009). *Meshfree methods: moving beyond the finite element method*. Taylor & Francis.
- Lu, P., Zhang, P. Q., Lee, H. P., Wang, C. M., & Reddy, J. N. (2007, December). Non-local elastic plate theories. In *Proceedings of the royal society of london a: Mathematical, physical and engineering sciences* (Vol. 463, No. 2088, pp. 3225-3240). The Royal Society.
- Malekzadeh, P., Setoodeh, A. R., & Beni, A. A. (2011a). Small scale effect on the free vibration of orthotropic arbitrary straight-sided quadrilateral nanoplates. *Composite Structures*, 93(7), 1631-1639.
- Malekzadeh, P., Setoodeh, A. R., & Beni, A. A. (2011b). Small scale effect on the thermal buckling of orthotropic arbitrary straight-sided quadrilateral nanoplates embedded in an elastic medium. *Composite Structures*, 93(8), 2083-2089.
- Martel, R., Schmidt, T., Shea, H. R., Hertel, T., & Avouris, P. (1998). Single-and multi-wall carbon nanotube field-effect transistors. *Applied physics letters*, 73(17), 2447-2449.
- Murmu, T., & Pradhan, S. C. (2009). Buckling analysis of a single-walled carbon nanotube embedded in an elastic medium based on nonlocal elasticity and Timoshenko beam theory and using DQM. *Physica E: Low-dimensional Systems and Nanostructures*, 41(7), 1232-1239.

- Murmu, T., & Pradhan, S. C. (2009). Buckling of biaxially compressed orthotropic plates at small scales. *Mechanics Research Communications*, 36(8), 933-938.
- Naderi, A., & Baradaran, G. H. (2013). Element free Galerkin method for static analysis of thin micro/nanoscale plates based on the nonlocal plate theory.
- Nowacki, W. (1974). The linear theory of micropolar elasticity. In *Micropolar Elasticity* (pp. 1-43).
- Peddeson, J., Buchanan, G. R., & McNitt, R. P. (2003). Application of nonlocal continuum models to nanotechnology. *International Journal of Engineering Science*, 41(3-5), 305-312.
- Pouresmaeli, S., Fazelzadeh, S. A., & Ghavanloo, E. (2012). Exact solution for nonlocal vibration of double-orthotropic nanoplates embedded in elastic medium. *Composites Part B: Engineering*, 43(8), 3384-3390.
- Pradhan, S. C., & Phadikar, J. K. (2009). Nonlocal elasticity theory for vibration of nanoplates. *Journal of Sound and Vibration*, 325(1-2), 206-223.
- Pumera, M., Ambrosi, A., Bonanni, A., Chng, E. L. K., & Poh, H. L. (2010). Graphene for electrochemical sensing and biosensing. *TrAC Trends in Analytical Chemistry*, 29(9), 954-965.
- Rao, C. N. R., Biswas, K., Subrahmanyam, K. S., & Govindaraj, A. (2009). Graphene, the new nanocarbon. *Journal of Materials Chemistry*, 19(17), 2457-2469.
- Reddy, J. N. (2010). Nonlocal nonlinear formulations for bending of classical and shear deformation theories of beams and plates. *International Journal of Engineering Science*, 48(11), 1507-1518.
- Sakhaee-Pour, A. (2009). Elastic properties of single-layered graphene sheet. *Solid State Communications*, 149(1-2), 91-95.
- Sakhaee-Pour, A., Ahmadian, M. T., & Vafai, A. (2008). Applications of single-layered graphene sheets as mass sensors and atomistic dust detectors. *Solid State Communications*, 145(4), 168-172.
- Samaei, A. T., Aliha, M. R. M., & Mirsayar, M. M. (2015). FREQUENCY ANALYSIS OF A GRAPHENE SHEET EMBEDDED IN AN ELASTIC MEDIUM WITH CONSIDERATION OF SMALL SCALE. *Materials Physics & Mechanics*, 22(2), 125-135.
- Shen, H. S. (2011). Nonlocal plate model for nonlinear analysis of thin films on elastic foundations in thermal environments. *Composite Structures*, 93(3), 1143-1152.
- Shen, L. E., Shen, H. S., & Zhang, C. L. (2010). Nonlocal plate model for nonlinear vibration of single layer graphene sheets in thermal environments. *Computational Materials Science*, 48(3), 680-685.
- Sobhy, M. (2014). Generalized two-variable plate theory for multi-layered graphene sheets with arbitrary boundary conditions. *Acta Mechanica*, 225(9), 2521-2538.
- Sobhy, M. (2014). Thermomechanical bending and free vibration of single-layered graphene sheets embedded in an elastic medium. *Physica E: Low-dimensional Systems and Nanostructures*, 56, 400-409.
- Wang, C. M., Tan, V. B. C., & Zhang, Y. Y. (2006). Timoshenko beam model for vibration analysis of multi-walled carbon nanotubes. *Journal of Sound and Vibration*, 294(4-5), 1060-1072.
- Wang, Q., & Varadan, V. K. (2006). Wave characteristics of carbon nanotubes. *International Journal of Solids and Structures*, 43(2), 254-265.
- Yang, F. A. C. M., Chong, A. C. M., Lam, D. C. C., & Tong, P. (2002). Couple stress based strain gradient theory for elasticity. *International Journal of Solids and Structures*, 39(10), 2731-2743.
- Zenkour, A. M., & Sobhy, M. (2013). Nonlocal elasticity theory for thermal buckling of nanoplates lying on Winkler–Pasternak elastic substrate medium. *Physica E: Low-dimensional Systems and Nanostructures*, 53, 251-259.
- Zhang, Y., Lei, Z. X., Zhang, L. W., Liew, K. M., & Yu, J. L. (2015). Nonlocal continuum model for vibration of single-layered graphene sheets based on the element-free kp-Ritz method. *Engineering Analysis with Boundary Elements*, 56, 90-97.



© 2018 by the authors; licensee Growing Science, Canada. This is an open access article distributed under the terms and conditions of the Creative Commons Attribution (CC-BY) license (<http://creativecommons.org/licenses/by/4.0/>).